separations

MDPI

Article

Targeted Offline Two-Dimensional HPLC and UHPLC-Orbitrap-MS Combined with Molecular Networking Reveal the Effect of Processing on Chemical Constituents of Xuetong (the Stem of *Kadsura heteroclita*)

Hanwen Yuan, Wei Su, Ling Liang, Qingling Xie, Mengying Lyu, Huanghe Yu, Bin Li and Wei Wang *

TCM and Ethnomedicine Innovation & Development International Laboratory, Innovative Material Medical Research Institute, School of Pharmacy, Hunan University of Chinese Medicine, Changsha 410208, China; hanwyuan@hnucm.edu.cn (H.Y.); suwei0310@163.com (W.S.); 20223695ll@stu.hnucm.edu.cn (L.L.); xieql12@126.com (Q.X.); dancytime@163.com (M.L.); yhh@hnucm.edu.cn (H.Y.); libin@hnucm.edu.cn (B.L.)
* Correspondence: wangwei402@hotmail.com

Abstract: Xuetong, the dried stem of *Kadsura heteroclita* (Roxb.) Craib, is a traditional Tujia medicine extensively used to treat rheumatoid arthritis (RA). All traditional Chinese medicines (TCMs) necessitate a processing stage called "Paozhi" before clinical application. However, there is a dearth of research concerning the processing methods employed for Xuetong. To investigate the impact of vinegar and wine processing on the chemical constituents of Xuetong, this study devised a targeted offline two-dimensional (2D) high-performance liquid chromatography (HPLC) and ultra-high-performance liquid chromatography-orbitrap mass spectrometry (UHPLC-orbitrap-MS) method. By incorporating various MS data-processing techniques, such as molecular networking technology, fragment-ion similarity searching (FISh), online and offline database matching, and fragmentation pattern analysis, a total of 158 components were identified in Xuetong. Among them, 14 were verified by comparison with the reference standards. Notably, aside from triterpenoids and lignans, catechin derivatives were found to be the predominant constituents of Xuetong, and their levels exhibited a significant decrease following processing. This method significantly improved peak capacity and resolution, overcoming the limitations of 1D LC in simultaneously analyzing highly polar catechin derivatives and less polar triterpenoids and lignans. Moreover, the developed method shows promise for Xuetong's quality control.

Keywords: two-dimensional HPLC; UHPLC-orbitrap-MS; molecular networking; *Kadsura heteroclita*; Paozhi

Citation: Yuan, H.; Su, W.; Liang, L.; Xie, Q.; Lyu, M.; Yu, H.; Li, B.; Wang, W. Targeted Offline Two-Dimensional HPLC and UHPLC-Orbitrap-MS Combined with Molecular Networking Reveal the Effect of Processing on Chemical Constituents of Xuetong (the Stem of *Kadsura heteroclita*). *Separations* **2024**, *11*, 87. https://doi.org/10.3390/separations11030087

Academic Editor: Magdalena Bartnik

Received: 28 February 2024
Revised: 13 March 2024
Accepted: 16 March 2024
Published: 18 March 2024

1. Introduction

A characteristic feature of traditional Chinese medicine (TCM) is the requirement for "Paozhi", a processing method that enhances efficacy or reduces toxicity before its clinical use [1]. Liquid adjuvants like vinegar and wine are often added during the processing of TCMs [2]. According to TCM theory, vinegar processing facilitates liver meridian absorption, relieving liver stagnation and promoting Qi circulation, while wine processing enhances blood circulation, resolves blood stasis, and nourishes the liver and kidneys [3]. Modern research supports the idea that wine processing enhances the anti-inflammatory effects, while vinegar processing strengthens the analgesic effects [4]. Although some studies have explored the chemical composition changes in processed medicinal materials, further comprehensive and in-depth analyses are needed [4,5].

Xuetong, the stem of *Kadsura heteroclita* (Roxb.) Craib, has the properties of dispelling wind and dampness, promoting blood circulation, and relieving pain [6]. It is widely utilized in Tujia ethnomedicine for treating rheumatoid arthritis (RA) [6]. The ethanol extract of Xuetong exhibited promising analgesic and anti-inflammatory properties [7].

It effectively reduced the levels of inflammatory factors such as TNF-α, IL-6, IL-17A, and IL-17F, thereby exerting a therapeutic effect on adjuvant-induced arthritis in rats [8]. We previously conducted a comprehensive investigation on the chemical constituents of Xuetong, isolating and identifying a total of 76 compounds, including 46 new ones [6]. Triterpenoids and dibenzocyclooctadiene pwere found to be its predominant components. Xuetongsu (schisanlactone E), a triterpenoid found in the highest concentration in Xuetong, has shown remarkable dose-dependent effects in terms of analgesia, anti-inflammatory properties, and anti-rheumatoid arthritis (RA) activity [9]. The dibenzocyclooctadiene in Xuetong has a protective effect on liver damage caused by various factors such as drugs, chemicals, alcohol, and viruses [10]. These components also showcase a diverse array of pharmacological activities, encompassing anti-inflammatory, analgesic, anti-HIV, anticancer, and anti-hepatitis B actions [6]. Currently, there is no available research exploring the impact of vinegar or wine processing on the efficacy of Xuetong. The specific alterations in its chemical composition resulting from these processing methods are still unknown.

One-dimensional high-performance liquid chromatography (1D HPLC) is widely used as the primary analytical method for quality control of TCMs, due to its high stability and reproducibility. However, it often fails to achieve baseline separation and provide sufficient resolution when analyzing complex samples. Two-dimensional LC integrates multiple separation mechanisms, such as reverse phase (C_{18}) liquid chromatography (RPLC), hydrophilic interaction chromatography (HILIC), and normal phase liquid chromatography (NPLC), which enable compounds to undergo dual separations, significantly enhancing both peak resolution and capacity [11,12]. Mass spectrometry (MS) techniques are widely employed for identifying the structure of natural products, but the complexity and vast amount of data pose challenges in data processing. Molecular networking compares MS/MS spectra and fragmentation patterns using vector-based computational algorithms. This approach visualizes highly similar components as an interconnected network, even without common fragment ions or neutral losses [13,14]. This feature enables the rapid and targeted identification of unknown compounds in complex MS data [15]. Other commonly used methods for MS data processing and compound structure identification include fragment-ion similarity searching (FISh), offline and online database matching, neutral loss searching (NLS), and mass defect filtering (MDF) [16–18].

This study successfully established an offline two-dimensional HPLC and UHPLC-orbitrap-MS method to target and identify the components in Xuetong separately. By integrating molecular networking, FISh, online and offline database matching, and fragmentation pattern analysis, 158 compounds were tentatively identified, with 14 being verified by comparison with the reference standards. The method is powerful for Xuetong's quality control. Interestingly, apart from the triterpenoids and lignans, this study revealed catechin derivatives as the principal constituents of Xuetong for the first time. It is worth noting that while the triterpenoids and lignans showed no consistent or significant changes during processing, the content of the catechin derivatives decreased significantly after vinegar processing and further decreased after wine processing. The finds are of significant importance for the scientific processing of Xuetong.

2. Materials and Methods

2.1. Chemicals and Reagents

HPLC-grade methanol and acetonitrile were procured from Sigma-Aldrich. Anpel Laboratory Technologies Inc. (Shanghai, China) and Tianjin Guangfu Fine Chemical Research Institute (Tianjin, China) provided the additives (phosphoric acid and formic acid, respectively) for the mobile phase. All aqueous solutions were prepared with C'estbon purified water (Shenzhen, China). Epigallocatechin, proanthocyanidin B4, and apigenin-5-*O*-*β*-D-glucopyranoside were obtained from Lemeitian Medicine (Chengdu, China). The other standards used in the study, including catechin, epigallocatechin, schizandriside, 6-hydroxyhinokini 6-*O*-*β*-D-glucopyranoside, 6-hydroxyhinokinin, heteroclitalactone E, heteroclitalactone G, *d*-epigalbacin, heteroclitalactone A, schisanlactone E, nigranoic acid,

heteroclitalactone F, schisandronic acid, and kadsurarin, were isolated from the extract of *Kadsura heteroclita*, as described in our previous research [6]. The four batches of stems of *Kadsura heteroclita* were collected from the Huping mountain area of Hunan in China.

2.2. Processing and Sample Solution Preparation

The raw material was sliced and air-dried to obtain crude Xuetong slices (CXT). The 50 g of CXT was mixed with 10 mL of Chinese rice wine (Huangjiu) and a suitable amount of H_2O. Following a 4 h soaking period, the mixture was subjected to stir-frying at 120 °C until slightly steaming. The stir-fried material was then shade-dried, producing wine-processed Xuetong (WXT). Similarly, 50 g of CXT was mixed with 20 mL of vinegar to obtain vinegar-processed Xuetong (VXT). The sample solution was prepared by mixing 0.5 g of sample powder with 10 mL of methanol in a 50 mL flask, followed by a 30 min ultrasonic extraction.

2.3. Targeted Offline 2D HPLC Separation

The first dimension (^{1}D) separation utilized a Fisher Wharton Xbridge C_{18} column (10 × 250 mm, 5 μm) on a Ruihe Tech B4 preparative HPLC system (Wuhan, China). Gradient elution was performed using acetonitrile (A) and H_2O with the following program: 0–15 min, 18% A; 15–20 min, 18–100% A; 20–35 min, 100% A, at a flow rate of 5 mL/min. A sample volume of 250 μL was injected, and the eluate was collected in two fractions. The fractions, F1 (3–16 min) and F2 (16–35 min), were concentrated using a rotary evaporator and reconstituted with 250 μL of methanol. The second dimension (^{2}D) separation of F1 and F2 was conducted on an Agilent HPLC 1260 system (Santa Clara, CA, USA) at a 1 mL/min flow rate. The detection wavelength was set at 210 nm, with sample injection volumes of 5 μL and 10 μL, respectively. The column temperatures were set at 45 °C and 20 °C, respectively. The mobile phase for both separations consisted of a 0.05 phosphate aqueous solution (A) and acetonitrile (B). The separation of F1 was performed using an Agilent Poroshell 120 HILIC-Z column (4.6 × 250 mm, 4 μm), employing a gradient elution program as follows: 0–10 min, 5–8% A; 10–15 min, 8% A; 15–88 min, 8–20% A. For the separation of F2, a Waters Atlantis T3 column (4.6 × 250 mm, 5 μm) was utilized, and the gradient elution program was as follows: 0–10 min, 20% B; 10–20 min, 20–25% B; 20–45 min, 25–42% B; 45–60 min, 60% B; 60–85 min, 60–95% B; 85–100 min, 95% B. The precision, stability, and repeatability of the 2D HPLC method were evaluated, following the methodology reported in the previous research [19]. In brief, the precision of the 2D HPLC method was assessed by repetitively measuring the same sample 6 times under identical conditions, with the relative standard deviation (RSD) serving as a measure. To determine its stability, the same sample was analyzed at various time points (0, 2, 4, 6, 8, and 12 h). Additionally, six parallel preparations of the same sample were made and subjected to analysis for repeatability evaluation.

2.4. ^{2}D UHPLC-MS Analysis

To analyze the impact of processing on minor components in Xuetong, F1 and F2 were subjected to ^{2}D LC-MS analysis using a Thermo Scientific Vanquish UHPLC and Orbitrap Exploris 120 system (Waltham, MA, USA). Equimolar mixtures of F1 and F2 from different sample batches were prepared as quality control (QC) samples to assess instrument stability, respectively. The mobile phase consisted of 0.05% formic acid aqueous solution (A) and acetonitrile (B) at a flow rate of 0.3 mL/min. The column temperature was maintained at 25 °C. F1 was analyzed using an Agilent Poroshell 120 HILIC-Z column (2.1 × 100 mm, 1.9 μm) with the following gradient elution program: 0–10 min, 95% B; 10–15 min, 95–92% B; 15–35 min, 92–80% B; 35–40 min, 80–40% B; 40–45 min, 40% B. F2 was analyzed using a Thermo Scientific Hypersil GOLDTM Aq-C_{18} column (2.1 × 100 mm, 1.9 μm) with the following gradient elution program: 0–10 min, 15–20% B; 10–35 min, 20–40% B; 35–45 min, 40–60% B; 45–80 min, 60–95% B; 80–90 min, 95% B.

The positive and negative ionization spray voltages were set at 3500 V and 2500 V, respectively. The sheath gas and aux gas flow rates were 50 and 10 Arb units, respectively. The ion transfer tube and vaporizer temperatures were 325 and 350 °C, respectively. Data-dependent acquisition (DDA) mode was used with an intensity threshold of 1.0×10^5. The full mass scan range was set to 100–1300 Da with an orbitrap resolution of 6000. The analysis was performed using a simultaneous acquisition method in both positive and negative ion modes. The intensity threshold for the MS2 scan was set at 1×10^5. Stepped higher-energy collisional dissociation (HCD) collision energy was set at 30, 60, and 90 eV.

2.5. Data Processing and Molecular Networking

The HPLC fingerprints were analyzed using the Similarity Evaluation System for Chromatographic Fingerprints of TCM (Version 2004 A). Principal component analysis (PCA) and partial least squares discriminant analysis (PLS-DA) were performed using Simca-p 17.0. All mass spectrometry data were imported into Compound Discoverer (CD) 3.3 for peak alignment, background subtraction, molecular networking analysis, and FISh. The online database mzCloud and the local database mzVault were used for the non-targeted identification of compounds in Xuetong. The peak area changes of catechin derivatives identified by 2D LC-MS were plotted using GraphPad Prism 10.

3. Results and Discussion

3.1. Optimization of the Targeted Offline 2D Chromatographic Conditions

The method 1D-LC is well-established for quality control in the traditional medicine industry. However, despite optimization efforts, the baseline separation of the major components of Xuetong could not be achieved using the 1D-LC method (Figure 1A and Figure S1 in the Supplementary Data). The chromatograms displayed significant baseline drift, and the peaks representing highly polar components showed unsatisfactory peak shapes characterized by excessive broadening. This was primarily attributed to the complex chemical composition of Xuetong, as well as the limited peak capacity of 1D HPLC. Furthermore, the highly polar compounds in Xuetong exhibited weak retention on the C_{18} chromatographic columns, challenging their effective separation.

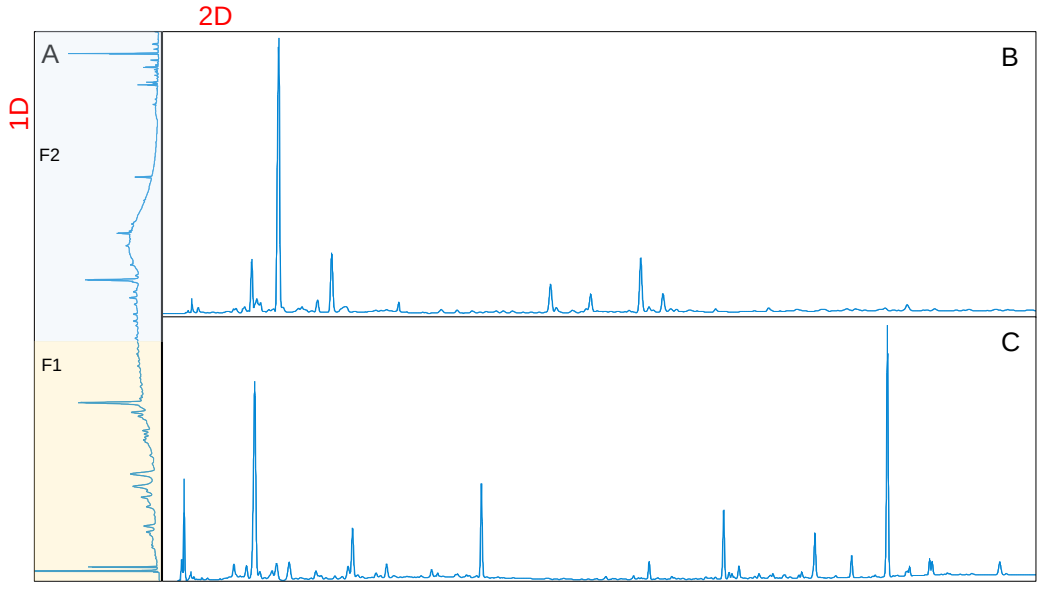

Figure 1. Optimized ^{1}D HPLC chromatogram of Xuetong (**A**) and ^{2}D HPLC separation of F1 (**B**) and F2 (**C**).

To address this challenge, preparative LC was initially employed to separate the sample into two fractions with significant polarity differences. Subsequently, C_{18} and HILIC-Z columns were utilized to separate the fractions. HILIC-Z offers a retention mechanism

similar to normal-phase chromatography, making it suitable for separating highly polar compounds. The chromatographic conditions were meticulously optimized, including injection volume, column temperature, mobile phase composition, and gradient elution program. The optimal conditions are outlined in Section 3.3, and the 2D separation of the samples is presented in Figure 1B,C. Conventional offline two-dimensional liquid chromatography methods emphasize the achievement of the highest possible separation of components by dividing the sample into multiple fractions for subsequent analysis. Nonetheless, these approaches are characterized by operational complexity, low reproducibility, and limited applicability in the quality control of TCM. Notably, our targeted offline two-dimensional liquid chromatography approach divided the 1D chromatogram into two fractions, ensuring effective separation of the significant components while maintaining practicality and reproducibility in the context of the TCM's quality control. The RSD values of all peak areas were below 6%, and all peak retention time RSD values were below 3%, demonstrating the stability and reliability of the method (Table 1).

Table 1. Method validation of the 2D HPLC separation system (n = 6, RSD, %).

Peaks	Peak Area			Retention Time		
	Precision	Stability	Repeatability	Precision	Stability	Repeatability
X1	2.479	2.359	2.531	1.428	1.683	1.534
X2	0.684	0.698	3.225	1.796	2.484	2.185
X3	5.372	2.391	2.789	1.970	1.767	2.002
X4	3.229	4.313	4.843	1.160	1.263	1.694
X5	1.225	1.097	5.006	1.006	1.188	1.620
X6	1.138	0.598	5.821	0.826	1.060	1.386
X7	2.573	2.941	5.603	0.683	1.145	1.395
Y3	1.134	1.533	3.798	0.948	0.071	0.492
Y7	2.035	1.313	4.155	0.326	0.034	0.321
Y8	0.699	1.266	2.892	0.080	0.019	0.328
Y9	4.531	1.265	4.543	0.037	0.010	0.072
Y10	5.012	1.172	4.498	0.016	0.009	0.093
Y13	1.159	1.025	6.592	0.015	0.007	0.050
Y14	1.472	1.393	4.400	0.017	0.007	0.015
Y15	1.526	1.306	2.493	0.019	0.005	0.050
Y16	2.312	1.221	5.273	0.020	0.004	0.031
Y18	6.521	3.594	4.681	0.034	0.005	0.089

3.2. Identification of the Major Compounds by Targeted 2D HPLC Method

The highly polar compounds in F1 were primarily catechin derivatives or their dimers. Through comparison with reference solutions, X2, X3, and X4 were identified as catechin, epigallocatechin, and proanthocyanidin B4, respectively (Figure 2). Based on the molecular formula and fragmentation patterns observed in subsequent MS analysis, it is tentatively suggested that X6 was anthocyanidin. However, due to its complex configuration, an exact identification could not be made without an available reference standard. Furthermore, X1 exhibited the same molecular formula and fragmentation patterns as schizandriside but with a significantly different retention time, indicating it was an isomer of schizandriside. In F2, the components mainly consisted of lignans and triterpenoids. By comparing with reference standards, the majority of which were previously isolated from Xuetong by our research group, a total of 12 compounds were identified. Similarly, subsequent MS analysis revealed the presence of multiple isomers of schizandriside in F2, such as Y1, Y2, Y4, and Y5. Y7 exhibited the same molecular formula and molecular weight as schizandriside but with fragment ions that were 18 Da less than that of schizandriside, suggesting it is also an isomer of schizandriside. Additionally, based on further MS analysis, Y10 was identified as heteroclitalactone L. Although this compound was isolated in our previous study, it is prone to dehydration to form heteroclitalactone G, making it difficult to compare with a reference standard for definitive identification [20].

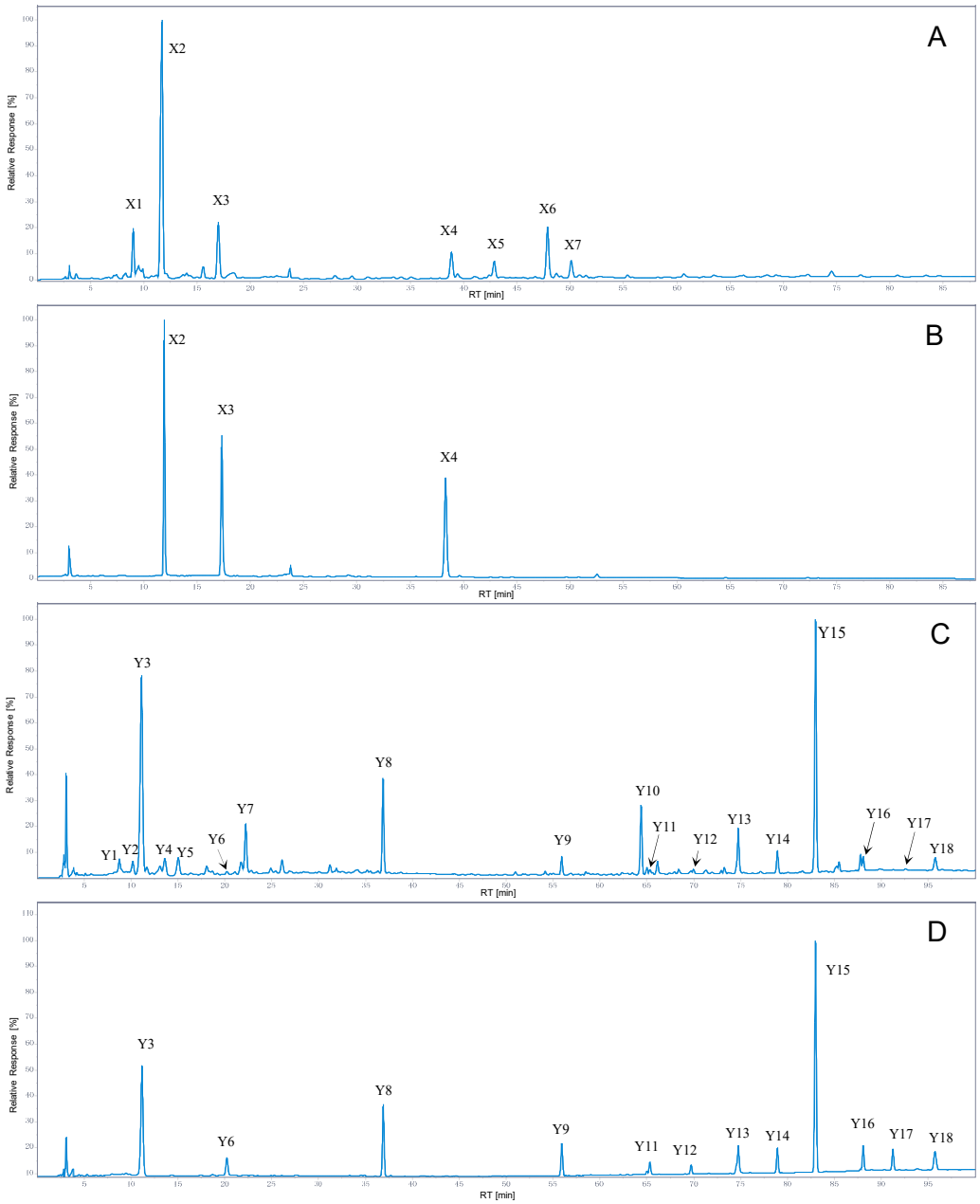

Figure 2. Comparison of ^{2}D HPLC chromatograms of F1 (**A**) and F2 (**C**) with the mixed standards solutions (**B**,**D**) (X2: catechin, X3: epigallocatechin, X4: proanthocyanidin B4, Y3: schizandriside, Y6: apigenin-5-*O*-*β*-D-glucopyranoside, Y8: 6-hydroxyhinokini 6-*O*-*β*-D-glucopyranoside, Y9: 6-hydroxyhinokinin, Y11: heteroclitalactone E, Y12: heteroclitalactone G, Y13: *d*-epigalbacin, Y14: heteroclitalactone A, Y15: schisanlactone E, Y16: nigranoic acid, Y17: heteroclitalactone F, Y18: schisandronic acid).

3.3. Compound Identification by ^{2}D UHPLC-MS

F1 and F2 were subjected to 2D UHPLC-MS analysis, and their total ion chromatograms (TIC) are visualized in Figure S2 of the Supplementary Data. PCA analysis of the peak areas of all features (Figure S3) showed tight clustering of all QC samples, confirming the method's stability and reliability. While Global Natural Products Social Molecular Networking (GNPS, https://gnps.ucsd.edu, accessed on 28 February 2024) is commonly used for molecular network analysis [21,22], its limitations in data conversion, computational power, and compound recognition were encountered in this study. Specifically, GNPS failed to recognize triterpenoids and cluster them into a molecular network in this study. In contrast,

Thermo Fisher's Compound Discoverer 3.3 (CD) software overcame these challenges with its robust computational capabilities and algorithms. CD seamlessly integrates with various data analysis methods, including online database (mzCloud) matching, FISh, and statistical analysis, enabling a comprehensive analysis of the LC-MS data. Therefore, in this study, CD was employed for molecular network analysis.

3.3.1. Identification of Catechin Derivatives and Phenols in F1

The molecular network of F1 is shown in Figure S4, where each node represents a compound. The pie chart for nodes was color-coded based on the proportion of the peak area of the precursor ion for each compound. According to the molecular networking, there were 22 catechin derivatives (Figure 3A), with CXT displaying significantly higher levels of each derivative compared to VXT and WXT. The fragmentation pattern of catechin was summarized, where the precursor ion initially lost one CO_2 molecule, generating a sub-ion at m/z 245.08193, or directly fragmented into smaller fragments such as m/z 179.03498, 123.04515, 109.02950, etc., (Figure 3C). Hydroxyl groups on the catechin were prone to substitution by other groups, which generally underwent fragmentation to yield a product ion at m/z 289.07176, representing the presence of catechin derivatives. Hence, this ion served as a diagnostic ion for these compounds. After employing FISh, 20 compounds (with class coverage of 100%) were scrutinized, 18 of which were components constituted by the molecular network (Figure 3B). This outcome underscored the efficacy of both methods in identifying catechin derivatives. Following the exclusion of in-source fragmentation, unmerged features, and compounds with uncomputable molecular formulas, 11 catechin derivatives were successfully identified based on their molecular formula and fragmentation pattern (Table S1). Among them, three were further confirmed using reference standards.

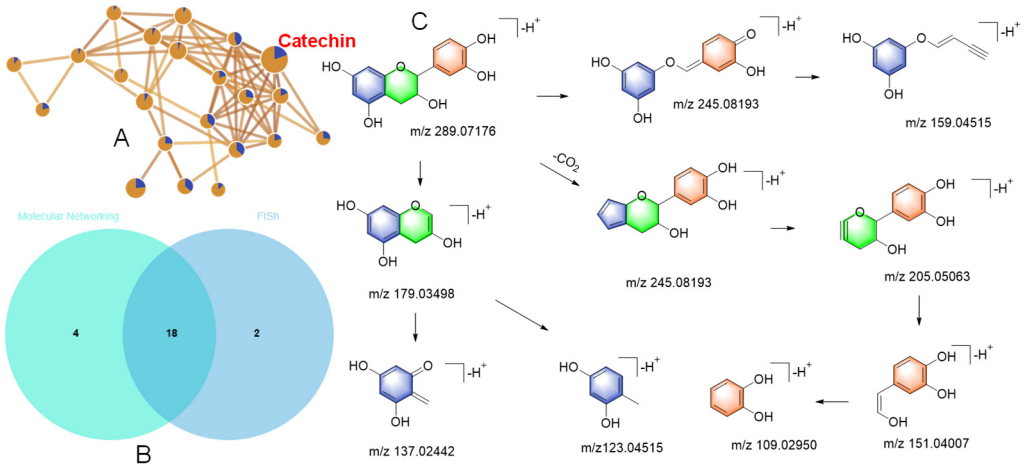

Figure 3. Molecular networking of catechin derivatives (**A**), Venn diagram of constituents by molecular networking and FISh (**B**), and proposed fragmentation pattern of catechin (**C**). The pie chart for nodes was color-coded based on the proportion of the peak area of the precursor ion for each compound: yellow (CXT), blue (VXT), and green (WXT).

F1 was found to contain a variety of phenols. However, there was no regular fragmentation pattern to follow for these compounds due to the diverse substituents and their varying positions. Therefore, the identification of these compounds primarily relied on mzCloud and mzVault. To ensure accurate identification, this study adopted a criterion where results with a best match of mzCloud or mzVault $\geq$85% and at least three major product ions matching the database records were deemed reliable. Using this approach, 26 phenols and 1 lignan were identified (Table S1). Furthermore, as mentioned in Section 2.2, an isomer of schizandriside was also found in F1. Therefore, 11 catechin derivatives, 26 phenols, and 2 lignans were identified from F1 (Table S1).

3.3.2. Identification of Lignan and Triterpenoid Derivatives in F2

In F2, with over 10,000 features, molecular networking proved effective in the targeted screening of potential compounds. Dibenzocyclooctadienes and triterpenoids responded well in the positive mode, with only a few lignans showing better responses in the negative mode. Thus, the positive and negative ion data sets were analyzed separately. Figure S5 shows a cluster of 45 features, potentially corresponding to dibenzocyclooctadienes. These compounds were identified using an in-house database compiled from previously identified dibenzocyclooctadienes in the *Schisandraceae* family, along with molecular formula and fragmentation patterns [10]. For example, compound **B31** displayed a $[M + Na]^+$ ion peak at m/z 595.21489, suggesting a molecular formula of $C_{30}H_{36}O_{11}$, consistent with kadsurarin in the in-house database. The MS^2 spectrum data also matched its fragmentation pattern (Figure 4). Its precursor ion $[M + Na]^+$ at 595.21498 lost the substituent at the C-7′ position to form an ion at m/z 435.14142. It could also undergo rearrangement by losing the substituent at the C-7′ position to generate the product ion at m/z 413.15948 and further produce additional fragment ions. Hence, compound **B31** was identified as kadsurarin. Overall, 25 dibenzocyclooctadienes were identified using this molecular networking approach (**B24**–**B49**, Table S2).

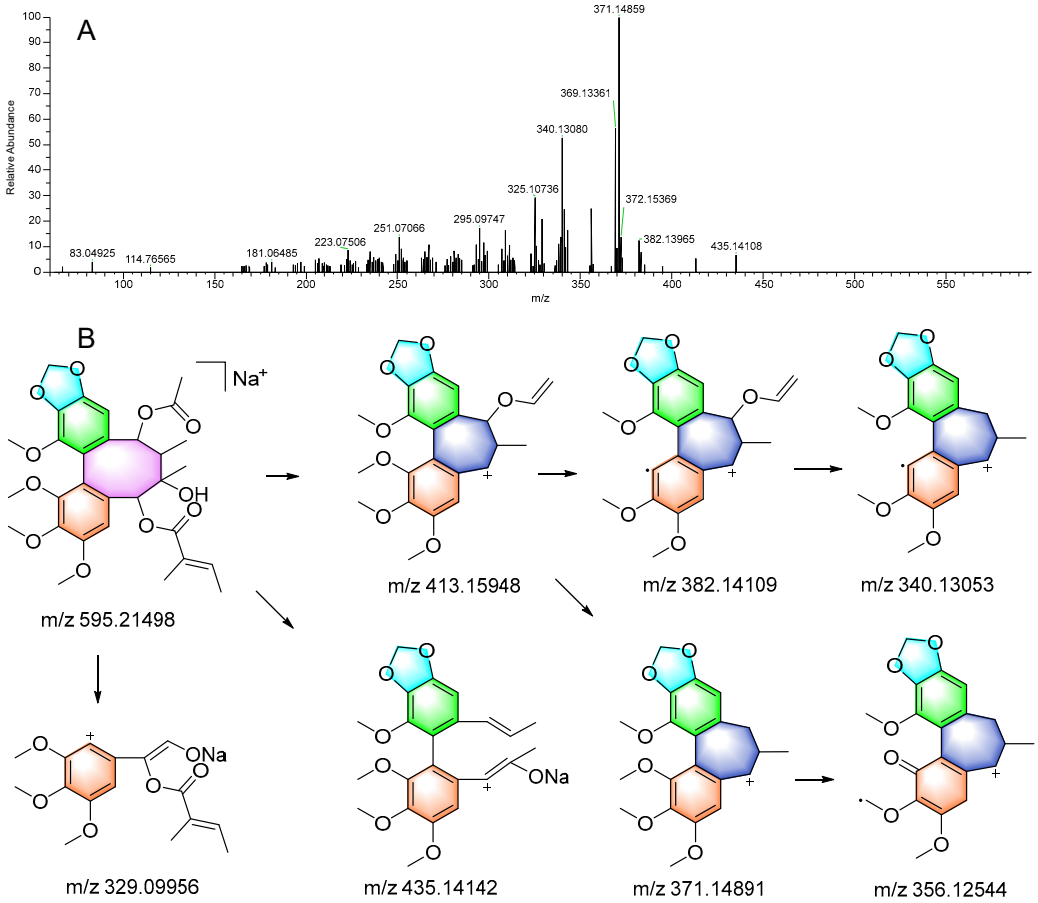

Figure 4. MS^2 spectrum (**A**) and proposed fragmentation pattern (**B**) of kadsurarin.

In addition, as mentioned in Section 2.2, other lignans, such as schizandriside, 6-hydroxyhinokinin, and 6-hydroxyhinokinin 6-*O*-*β*-D-glucopyranoside, were detected in Xuetong. These lignans showed a more pronounced response in the negative mode. The FISh analysis, utilizing the diagnostic ions for schizandriside and 6-hydroxyhinokinin (m/z 369.09798 and m/z 359.15001, respectively), resulted in the retrieval of 49 components. Among them, the molecular network containing schizandriside in the negative mode consisted of 14 compounds, with 9 compounds searched by FISh. Similarly, the molecular

network of 6-hydroxyhinokinin had 10 compounds, with 6 compounds searched by FISh. FISh exhibited heightened sensitivity in detecting these lignans, although false-positive results were possible. By analyzing the molecular formula and fragmentation patterns, a preliminary identification of 23 components was achieved, including 8 derivatives of schizandriside (**B1**–**B8**) and 15 derivatives of 6-hydroxyhinokinin (**B9**–**B23**, Table S2). Significantly, this study unveiled seven lignan glycosides in Xuetong, featuring two sugar moieties, which could potentially be new compounds. This was the first time compounds with two sugar moieties have been found in Xuetong. Compound **B9** was identified as a lignan glycoside with one attached glucose based on its MS^2 data. Its aglycone possessed one additional molecule of H_2O compared to 6-hydroxyhinokinin, suggesting its structure as 8-hydroxyoxomatairesinol-*β*-D-glucopyranoside, which is also a new compound. Additionally, apigenin 5-*O*-*β*-D-glucopyranoside, discussed in Section 2.2, was detected in Xuetong and exhibited a strong response in negative mode.

For the identification of triterpenoids in Xuetong, this study employed a molecular networking approach. Among them, schisanlactone E was found to be the most abundant triterpenoid in Xuetong, forming a molecular network consisting of 100 triterpenoid components. Due to the complexity of triterpenoid structures and the similarity in their fragmentation patterns, it was challenging to directly determine the structures of individual compounds based on their fragmentation patterns. This study created an in-house database by compiling isolated triterpenoid compounds from Xuetong [6]. By matching these compounds with the in-house database and online databases such as mzCloud and evaluating the consistency of their MS^2 spectra with the fragmentation patterns of corresponding compounds, a total of 70 components were successfully identified among the 100 compounds (Table S3). Among them, the structures of eight compounds were confirmed through comparison with the standards.

3.4. Effect of Processing on the Constituents of Xuetong

As shown in the fingerprints (Figure S6), processing had no impact on triterpenoid and lignan levels in the Xuetong sample. However, catechin compounds (X2–X7) noticeably decreased in content after processing. No distinct differences in chemical composition were observed between vinegar-processed and wine-processed samples. These results were further confirmed by PLS-DA analysis (Figure 5), where significant differences were observed between unprocessed (CXT) and processed samples (WXT and VXT) for the major components in F1.

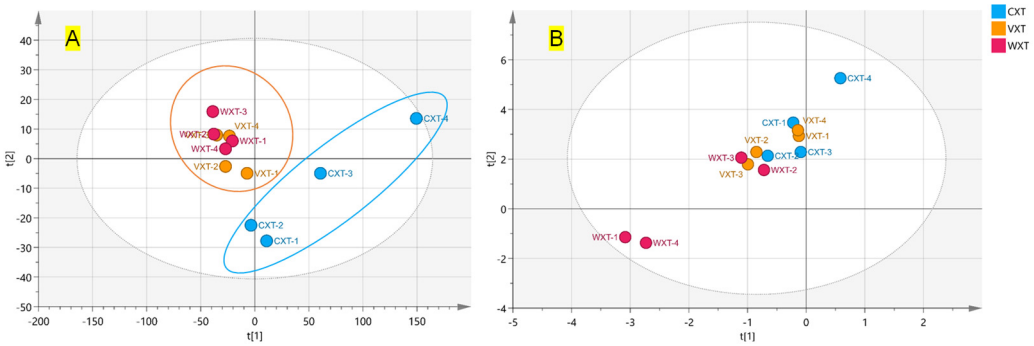

Figure 5. PLS–DA scoring plot of 2D HPLC data of F1 (**A**) and F2 (**B**).

PLS-DA analysis of all compounds identified through ^{2}D LC-MS revealed distinct separation trends between pre- and post-processing samples (Figure 6A). Particularly, significant differences were observed in the chemical compositions of wine-processed and vinegar-processed Xuetong, indicating the influence of different adjuvants on the processing of Xuetong. Further PLS-DA analysis focused on the top 10 compounds with the highest variable importance projection (VIP) values (Figure 6B), clearly distinguishing the three sample groups. Notably, the majority of these compounds were catechin derivatives.

The analysis of these 11 catechin derivatives showed a significant decrease in peak area after vinegar processing (Figure 7), followed by a further decrease after wine processing. No significant patterns of change were observed for other compound types. These systematic content changes may play a vital role in the altered therapeutic effects of processed Xuetong.

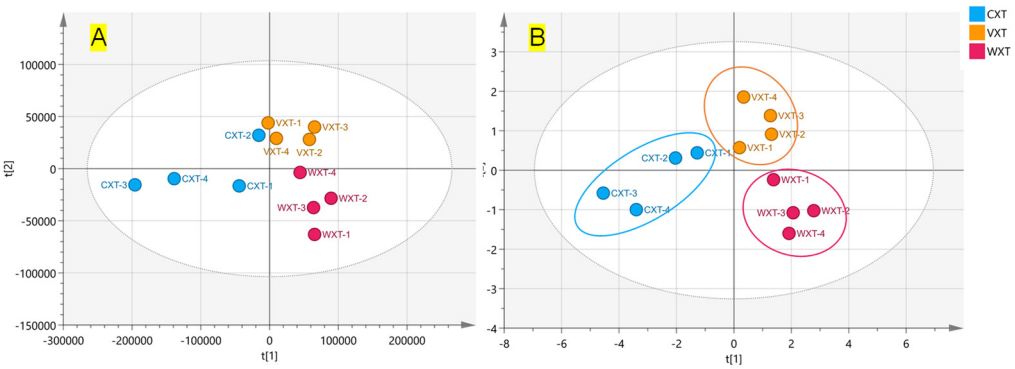

Figure 6. PLS-DA scoring plot of all compounds identified by ^{2}D LC-MS analysis (**A**) and top 10 important variables according to the VIP scores (**B**).

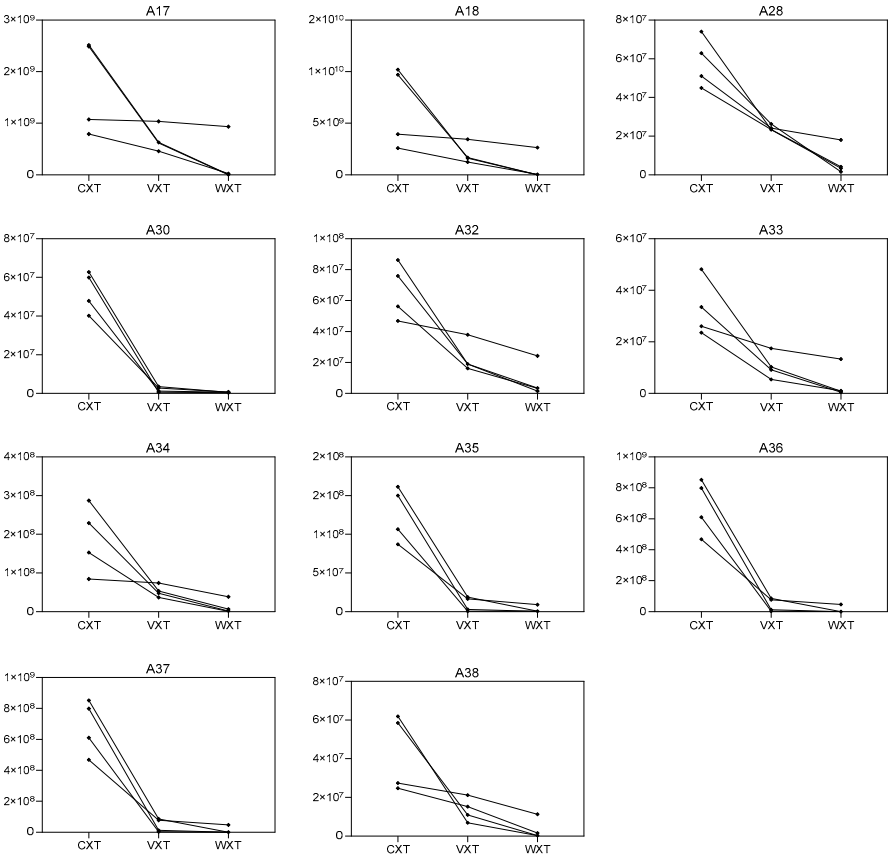

Figure 7. Effects of processing on the peak area of 11 catechin derivatives in Xuetong.

4. Conclusions

This study established a targeted 2D HPLC and UHPLC-MS method for analyzing the components of Xuetong. It employed various techniques, including molecular networking, FISh analysis, mzCloud, fragmentation patterns, and an in-house database, to identify the constituents. A total of 158 components were identified, primarily catechin derivatives, phenols, lignans, and triterpenoids. This study is the first to discover that catechin derivatives are also major components of Xuetong; they exhibited high polarity and could not be

baseline separated using conventional C_{18} columns. The targeted 2D HPLC and UHPLC-MS utilized in this study effectively achieved their separation. Catechin derivatives exhibit a diverse range of pharmacological effects, such as anti-inflammatory, cytotoxic, antioxidative, and osteoprotective properties. However, further research is needed to ascertain whether these components possess anti-RA activity or if they interact synergistically with other constituents in Xuetong. As another crucial component of Xuetong, the catechin derivatives should not be overlooked in future studies focusing on this substance's chemical composition, pharmacology, and quality control.

Processing is a characteristic feature of TCM, and wine and vinegar processing are known to enhance the Qi-promoting and analgesic effects. Xuetong is traditionally used for treating rheumatoid arthritis due to its Qi-promoting and analgesic properties. This study investigated the impact of wine and vinegar processing on the constituents of Xuetong. It found that the content of catechin derivatives significantly decreased after vinegar processing and further decreased after wine processing. However, no significant changes were observed in the other two major class compounds (lignans and triterpenoids). The changes in catechin derivatives may be attributed to their relatively lower stability compared to triterpenoids and lignans, making them more susceptible to decomposition under heating conditions. The consistent temperature during the vinegar and wine processing led to noticeable variations in the catechin content. This suggests that the acetic acid or ethanol underwent distinct chemical reactions with the catechin components at high temperatures, resulting in inconsistent decomposition rates for catechin compounds. The investigation into the changes in the catechin derivatives during processing may provide insights for future studies on the impact of processing on the anti-RA activity of Xuetong, as well as research on the processing mechanism. These findings offer valuable references and scientific evidence to improve the scientific processing of Xuetong. Moreover, the developed targeted 2D HPLC and UHPLC-MS methods in this study hold significant importance for the quality control and standardization of Xuetong.

Supplementary Materials: The following supporting information can be downloaded at: https://www.mdpi.com/article/10.3390/separations11030087/s1, Figure S1: Optimized 1D HPLC chromatogram of Xuetong; Figure S2: Total ion chromatogram (TIC) in the positive model of F1 (A) and F2 (B); Figure S3. PCA scoring plot of 2D LC-MS data of F1 (A) and F2 (B); Figure S4. Molecular networking constructed by 2D UHPLC-MS data of F1; Figure S5. Molecular networking constructed by 2D UHPLC-MS data of F2 in positive mode; Figure S6. 2D HPLC Fingerprints of F1 (A) and F2 (B) of RXT (S9–S12), VXT (S5–S8), and WXT (S1–S4); Table S1. Compound identification of F1 by 2D UHPLC-MS analysis; Table S2. Lignans in F2 identified by 2D UHPLC-MS analysis; Table S3. Triterpenoids in F2 identified by 2D UHPLC-MS analysis.

Author Contributions: Data curation, M.L.; investigation, H.Y. (Hanwen Yuan), L.L. and Q.X.; software, Q.X.; writing—original draft preparation, H.Y. (Huanghe Yu); writing—review and editing, W.S., B.L. and W.W. All authors have read and agreed to the published version of the manuscript.

Funding: This research was funded by the National Natural Science Foundation of China (82304878 and 82204766), Natural Science Foundation of Hunan province (2022JJ40318 and 2023JJ40490), the Scientific Research Fund of Hunan University of Chinese Medicine (2021XJJJ006), and Xiaohe Sci-Tech Talents Special Funding under Hunan Provincial Sci-Tech Talents Sponsorship Program (2023TJ-X71), Scientific Research Project of Hunan Provincial Education Department (21B0394), Research Project of Hunan Administration of Traditional Chinese Medicine (B2023055), and Outstanding Youth Program of Hunan University of Chinese Medicine (202202).

Data Availability Statement: The data presented in this study are available upon reasonable request from the corresponding authors.

Conflicts of Interest: The authors declare no conflicts of interest.

References

1. Hou, A.; Lv, J.; Zhang, S.; Zhang, J.; Yang, L.; Jiang, H.; Kuang, H. Salt processing: A unique and classic technology for Chinese medicine processing. *Front. Pharmacol.* **2023**, *14*, 116047. [CrossRef]
2. Li, R.; Zhang, Q.; Liu, J.; He, L.; Huang, Q.; Peng, W.; Wu, C. Processing methods and mechanisms for alkaloid-rich Chinese herbal medicines: A review. *J. Integr. Med.* **2021**, *19*, 89–103. [CrossRef]
3. Chen, L.; Verpoorte, R.; Yen, H.; Peng, W.; Cheng, Y.; Chao, J.; Pao, L. Effects of processing adjuvants on traditional Chinese herbs. *J. Food Drug Anal.* **2018**, *26*, S96–S114. [CrossRef]
4. Chen, Z.; Ye, S.; Zhu, R. The extraordinary transformation of traditional Chinese medicine: Processing with liquid excipients. *Pharm. Biol.* **2020**, *58*, 561–573. [CrossRef]
5. Zhan, Z.; Yang, L.; Zhang, Q.; Jialuo, C.; Deng, G.; Ouyang, L.; Wu, P. Present situation and emerging problems of processing Chinese materia medica. *China J. Tradit. Chin. Med. Pharm.* **2018**, *33*, 3233–3238.
6. Wang, M.; Jiang, S.; Yuan, H.; Zafar, S.; Hussain, N.; Jian, Y.; Li, B.; Gong, L.; Peng, C.; Liu, C.; et al. A review of the phytochemistry and pharmacology of *Kadsura heteroclita*, an important plant in Tujia ethnomedicine. *J. Ethnopharmacol.* **2021**, *268*, 113567. [CrossRef] [PubMed]
7. Yu, H.; Lin, Y.; Zeng, R.; Li, X.; Zhang, T.; Tasneem, S.; Chen, C.; Qiu, Y.; Li, B.; Liao, J.; et al. Analgesic and anti-inflammatory effects and molecular mechanisms of *Kadsura heteroclita* stems, an anti-arthritic Chinese Tujia ethnomedicinal herb. *J. Ethnopharmacol.* **2019**, *238*, 111902. [CrossRef] [PubMed]
8. Yu, H.; Zeng, R.; Lin, Y.; Li, X.; Tasneem, S.; Yang, Z.; Qiu, Y.; Li, B.; Wang, Y.; Cai, X.; et al. *Kadsura heteroclita* stem suppresses the onset and progression of adjuvant-induced arthritis in rats. *Phytomedicine* **2019**, *58*, 152876. [CrossRef]
9. Yu, H.; Fan, J.; Shehla, N.; Qiu, Y.; Lin, Y.; Wang, Z.; Cao, L.; Li, B.; Daniyal, M.; Qin, Y.; et al. Biomimetic hybrid membrane-coated xuetongsu assisted with laser irradiation for efficient rheumatoid arthritis therapy. *ACS Nano* **2022**, *16*, 502–521. [CrossRef] [PubMed]
10. Liu, S.; Yang, Y.; Hussain, N.; Jian, Y.; Li, B.; Qiu, Y.; Yu, H.; Wang, H.; Wang, W. Dibenzocyclooctadiene lignans from the family Schisandraceae: A review of phytochemistry, structure-activity relationship, and hepatoprotective effects. *Pharmacol. Res.* **2023**, *195*, 106872. [CrossRef] [PubMed]
11. Zhang, Z.; Xu, Y.; Shen, A.; Fu, D.; Liu, D.; Liu, Y.; Liang, X. Offline two-dimensional normal-phase × reversed-phase liquid chromatography coupled with high-resolution mass spectrometry for comprehensive analysis of chemical constituents in *Euphorbia kansui*. *J. Chromatogr.* **2023**, *1693*, 463897. [CrossRef]
12. Zuo, T.; Zhang, C.; Li, W.; Wang, H.; Hu, Y.; Yang, W.; Jia, L.; Wang, X.; Gao, X.; Guo, D. Offline two-dimensional liquid chromatography coupled with ion mobility-quadrupole time-of-flight mass spectrometry enabling four-dimensional separation and characterization of the multicomponents from white ginseng and red ginseng. *J. Pharm. Anal.* **2020**, *10*, 597–609. [CrossRef]
13. Messaili, S.; Colas, C.; Fougère, L.; Destandau, E. Combination of molecular network and centrifugal partition chromatography fractionation for targeting and identifying *Artemisia annua* L. antioxidant compounds. *J. Chromatogr.* **2020**, *1615*, 460785. [CrossRef]
14. Qin, G.-F.; Zhang, X.; Zhu, F.; Huo, Z.-Q.; Yao, Q.-Q.; Feng, Q.; Liu, Z.; Zhang, G.-M.; Yao, J.-C.; Liang, H.-B. MS/MS-based molecular networking: An efficient approach for natural products dereplication. *Molecules* **2023**, *28*, 157. [CrossRef]
15. Yu, J.S.; Seo, H.; Kim, G.B.; Hong, J.; Yoo, H.H. MS-based molecular networking of designer drugs as an approach for the detection of unknown derivatives for forensic and doping applications: A case of NBOMe derivatives. *Anal. Chem.* **2019**, *91*, 5483–5488. [CrossRef] [PubMed]
16. Parailloux, M.; Godin, S.; Lobinski, R. Nontargeted screening for flavonoids in *Salicornia* plant by reversed-phase liquid chromatography-electrospray orbitrap data-dependent MS^2/MS^3. *Molecules* **2023**, *28*, 3022. [CrossRef]
17. Yu, Y.; Yao, C.; Guo, D. Insight into chemical basis of traditional Chinese medicine based on the state-of-the-art techniques of liquid chromatography−mass spectrometry. *Acta Pharm. Sin. B* **2021**, *11*, 1469–1492. [CrossRef]
18. Yu, Y.; Yao, C.; Wei, W.; Li, H.; Huang, Y.; Yao, S.; Qu, H.; Chen, Q.; Mei, Q.; Wu, W.; et al. Integration of offline two-dimensional chromatography and mass defect filtering-based precursor ion list data acquisition for targeted characterization of diterpenoid alkaloids in the lateral roots of *Aconitum carmichaelii*. *J. Chromatogr.* **2022**, *1684*, 463554. [CrossRef]
19. Han, C.; Chen, J.; Chen, B.; Sen-Chun Lee, F.; Wang, X. Fingerprint chromatogram analysis of *Pseudostellaria heterophylla* (Miq.) Pax root by high performance liquid chromatography. *J. Sep. Sci.* **2006**, *29*, 2197–2202. [CrossRef] [PubMed]
20. Wang, W.; Xu, Z.; Yang, M.; Liu, R.; Wang, W.; Liu, P.; Guo, D. Structural determination of seven new triterpenoids from *Kadsura heteroclita* by NMR techniques. *Magn. Reson. Chem.* **2007**, *45*, 522–526. [CrossRef] [PubMed]
21. Baskiyar, S.; Ren, C.; Heck, K.L.; Hall, A.M.; Gulfam, M.; Packer, S.; Seals, C.D.; Calderón, A.I. Bioactive natural products identification using automation of molecular networking software. *J. Chem. Inf. Model.* **2022**, *62*, 6378–6385. [CrossRef] [PubMed]
22. Caldas, L.A.; Zied, D.C.; Sartorelli, P. Dereplication of extracts from nutraceutical mushrooms *Pleurotus* using molecular network approach. *Food Chem.* **2022**, *370*, 131019. [CrossRef] [PubMed]